

1 High-multiplicity neutron events 2 registered by NEMESIS experiment

3 **M. Kasztelan,^{a,*} T. Enqvist,^b K. Jędrzejczak,^a J. Joutsenvaara,^d O. Kotavaara,^d**
4 **P. Kuusiniemi,^b K.K. Loo,^f J. Orzechowski,^a J. Puputti,^d A. Sobkow,^a M. Słupecki,^e**
5 **J. Szabelski,^a I. Usoskin,^c W.H. Trzaska^b and T.E. Ward^{g,h}**

6 ^aNational Centre for Nuclear Research, 28 Pułku Strzelców Kaniowskich 69, Łódź, Poland

7 ^bDepartment of Physics, University of Jyväskylä, P.O. Box 35, FI-40014 University of Jyväskylä, Finland

8 ^cUniversity of Oulu, Sodankyla Geophysical Observatory, P.O. Box 3000, FIN-99600 Sodankyla, Finland

9 ^dUniversity of Oulu, Kerttu Saalasti Institute, Pajatie 5, 85500 Nivala, Finland

10 ^eHelsinki Institute of Physics (HIP), P.O. Box 64, 00014 University of Helsinki, Finland

11 ^fInstitut für Physik (IPH), Johannes Gutenberg-Universität Mainz (JGU), Staudingerweg 7, 55128
12 Mainz, Germany

13 ^gHigh Energy Physics (HEP), U.S. Department of Energy, SC-25/Germantown Building, 1000
14 Independence Ave., SW, Washington, D.C., 20585, United States

15 ^hTechSource, Santa Fe, NM, United States

16 E-mail: marcin.kasztelan@ncbj.gov.pl

17 Neutron-induced interactions contribute to the signal-mimicking background in deep-underground searches for exotic phenomena such as Dark Matter, neutrino-less double beta decay, proton decay, etc. Apart from radioactive decay, the primary source of neutrons underground are high-energy muons from cosmic showers. While the maximum number of fission neutrons is around six and energies around one MeV, muon-induced interactions may generate hundreds of neutrons, also with high energies. Furthermore, these processes are not yet reproduced in numerical simulations with sufficient reliability. The main goal of the NEMESIS experiment is to improve our knowledge and understanding of cosmic muon-induced neutron production in high-Z targets. NEMESIS (New Emma MEasurementS Including neutronS) is taking data at a depth of 210 m.w.e. in Callio Lab in the Pyhäsalmi mine, Finland.

37th International Cosmic Ray Conference (ICRC 2021)
July 12th – 23rd, 2021
Online – Berlin, Germany

*Presenter

1. Introduction

Neutron flux in underground experiment vicinity is important for estimation of background for different studies. Contributing neutrons are from different fission reactions in surrounding rock etc., and from neutron-induced interactions. A fission reaction produces about six neutrons with energies around one MeV. In muon-induced interactions may generate hundreds of neutrons, and with higher energies. Results of that process is not well reproduced in computer simulations. The main goal of the NEMESIS experiment is to measure multi-neutron events occurring in muon interactions in different targets. In this work results obtained from lead target are presented. NEMESIS (New Emma MEasurementS Including neutronS) is taking data at a depth of 210 m.w.e. (75m) in Callio Lab [1] at the Pyhäsalmi mine [2] in Finland since November 2019.

The neutron setup consists of fourteen ^3He counters placed in polyethylene blocks. Data from the helium counters and muon scintillation detectors are collected by F/E electronics digitizing waveforms signals. Waveforms are long enough to include muons and delayed neutron signals from helium counters. The presented neutron multiplicity spectra shown here include a 349-day (live time) run with a 565 kg Pb target, a 166-day run without the target, and the outcome of the relevant Geant4 simulations. The neutron multiplicity spectrum shows a linear behavior on a doubly logarithmic scale. The largest registered event had 33 identified neutrons. For that event, correcting for nearly 8% detection efficiency, determined with Geant4, the required neutron emission is around 400 neutrons. The origin of such a large multiplicity of neutrons is still not known.

2. The first NEMESIS setup

The first NEMESIS setup is shown schematically in Fig.1 and the photo of it's central part in Fig.2. The first NEMESIS setup is a demonstrator of full-size NEMESIS Dark Matter experiment and uses the EMMA infrastructure [3] together with the Roland Maze outreach project detectors [4]. This solution allows for the combination of muon tracking with the position-sensitive registration of neutrons. This gives us a muon-induced neutron spectra, yielding muon-induced neutron spectra, neutron production yields, and lateral distributions for the observed high-multiplicity events (in one dimension).

The main element of the setup is the array of fourteen proportional counters [5] filled with 4 atm. ^3He gas and placed in polyethylene (PE) blocks. The helium counters were produced by ZdAJ [6]. Polyethylene acts as a moderator, increasing neutron capture efficiently by ^3He nuclei. NEMESIS helium counters has been previously used for neutron background measurements in several European underground laboratories [7–9] as part of the ILIAS and BSUIN projects [10]. A custom-made neutron acquisition system (NDAQ) collects data from ^3He detectors and two 1m^2 amplitude-sensitive scintillation detectors.

The muon-tracking part of the setup (Fig.1) consist of 46 SC16 [3] scintillator EMMA modules forming a 5-layer, 736-pixel muon telescope. The SC16 modules were designed for extended use underground. They were used, for instance, to measure muon flux at LSC in Canfranc [11]. Each SC16 has a $50 \times 50 \text{ cm}^2$ footprint and consist 16 individual pixels ($12.5 \times 12.5 \times 3.0 \text{ cm}^3$). Each module have one common time and one hit-pattern output [12]. These pixelized detectors worked in hodoscopic mode. Data from the muon telescope are collected by a separate data acquisition

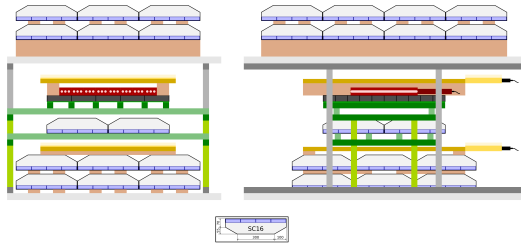


Figure 1: Our detector set-up: Front and side views. System is operating from November 2019. EMMA hodoscopic detectors (in grey) form 5 layers. Dark gray layer in the center is made of 5cm lead bricks. Above it there are polyethylene blocks with 14 helium neutron counters (in white holes). Yellow layers are 2 scintillation detectors $1m^2$ each.

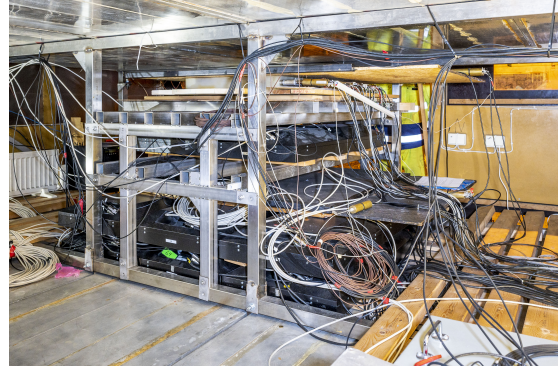


Figure 2: Photo of central part of first NEMESIS setup.

58 system (EMMA DAQ) requiring offline clock synchronization procedure with NDAQ. EMMA DAQ
 59 is triggered when at least one of two top layers and at least one from bottom layers of SC16 have
 60 signals in coincidence.

61 Neutron detectors generate the main
 62 NEMESIS trigger. The NDAQ frontend elec-
 63 tronic modules distribute the trigger to all
 64 channels via a common bus. Each helium
 65 counter triggers all the others and the two Maze
 66 Project scintillators. All signals are recorded
 67 by NDAQ. Data are collected as waveforms
 68 for further offline analysis. For each event, a
 69 clock synchronization signal is send to EMMA
 70 DAQ. NDAQ consist a 8-bit analogue-to-digital
 71 converters (ADC) coupled to circular memory
 72 buffer with 2k ADC samples. A signal sam-
 73 pling frequency of 1 MHz is appropriate for the current detection requirements. Data are transferred
 74 via a USB to the local PC, where they are stored as ROOT files [13]. To increase the dynamic range,
 75 each $1m^2$ scintillator detector provides two waveform signals, one from PMT's anode, and ~ 30
 76 times weaker signal from the 6^{th} dynode. The waveforms are stored by the frontend electronics
 77 (FE) in 2 ms circular buffers. The first $350\mu s$ precede the neutron trigger to capture the prompt
 78 muon signal in the scintillation detectors, accounting for neutron thermalization time. Neutrons
 79 use on average about $50\mu s$ for thermalization before their registration. The rest of waveform may
 80 include signals from subsequent neutrons, arriving with a delay caused by the time spread of the
 81 thermalization process.

82 The first NEMESIS run lasted 349 days. The 565 kg Pb target consisted of fifty standard Pb
 83 bricks, $20 \times 10 \times 5 cm^3$ each, forming a $1m^2$, 5 cm thick, uniform layer. Subsequently, the lead
 84 was removed for 7-month background measurement. From August, we intend to run with a copper
 85 target.

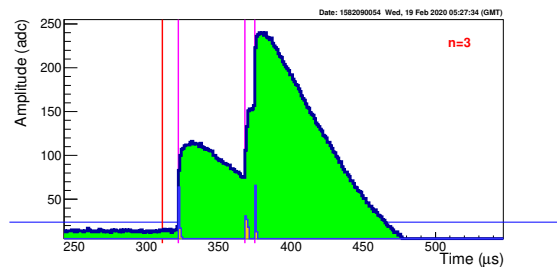


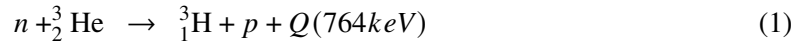
Figure 3: Example of multiple neutron signal registered in single 3He counter with identified 3 neutrons. Only fraction of whole registered wave-form is shown to visualize the structure of neutron signals.

86 In high-multiplicity events, the neutron signals may overlap, making them difficult to distinguish
 87 and count correctly, resulting in efficiency loss. The example in Fig.3 is relatively easy to interpret.
 88 However, overflow signals are often encountered with large neutron multiplicities. We are improving
 89 the detection method for the NEMESIS upgrade, including better software, higher sampling rate,
 90 higher dynamics of amplitude measurements, and additional helium counters. Also considered are
 91 improvements in muon tracking and passive shield against neutron flux from the surrounding rock.
 92 These measures will increase registration efficiency and lower the background.

93 3. Research methodology

94 Following a neutron capture by a ${}^3\text{He}$ nucleus (eq.1), the reaction products are emitted in
 95 opposite directions. Due to negligible kinetic energy of the primary neutron, there is no need to
 96 correct for the centre of mass velocity. The so called "wall-effect" [5], visible in the amplitude
 97 spectrum (Fig.6), appears when either the proton or tritium produced in the capture reaction escapes
 98 from the active volume of the counter before depositing their total energy. For non relativistic
 99 neutrons ($E_n < 100 \text{ keV}$), capture cross section is inversely proportional to the neutron velocity.
 100 For neutron witch energies from 10^{-5} to 10^4 eV that relation can be parameterized as follows:
 101 $\sigma(E_n/\text{barn}) = 847 E_n^{-0.5}[\text{eV}]$.

102 Used nuclear reaction to detect neutrons:



103 NEMESIS neutron identification proceeds in stages. All analysis was done offline. First
 104 waveform differences between consecutive ADC samples are calculated. This is depicted by the
 105 orange inset in Fig.3. The waveforms are scanned for signals exceeding a selected threshold. The
 106 corresponding ADC channel provides a reference for the registration time. The value resulting from
 107 adding three consecutive differences is proportional to the amplitude of the measured signal. The
 108 second important parameter is the largest difference in the vicinity of the potential signal. This
 109 value is proportional to the rise time of the registered pulse. The rise time was used for selecting
 110 neutron signals, as shown in Fig.5.

111 Data collected by our USB interface required clustering. Then, a search for potential signals in
 112 the waveform was performed. Next, neutron signals were identified through cuts on the amplitude
 113 and maximum derivative between the consecutive ADC samples. The procedure is illustrated in
 114 Fig.5. Proper neutron signals are inside the triangular area delimited by the cut lines.

115 The selection procedure is carried out for each counter separately after selecting the appropriate
 116 cuts presented in Fig. 5. Cutting lines have different tasks. The red line eliminates low amplitude
 117 signals caused by electronic noise and contributions from the large amount of gamma photons
 118 recorded in the counter (in some cases). The blue line rejects signals with higher amplitudes which
 119 are come from alpha particles of the helium counter's own radioactivity. Our own radioactivity
 120 of helium counters is at the level $0.78 \text{ MeV}^{-1}\text{h}^{-1}$. These alpha particles are emitted inwards the
 121 counter from the housing material as a result of decays from natural radioactivity chains. The green
 122 line eliminates potential signals from high voltage leakage appearing as a result of a bit "unclean"
 123 in the HV-BNC connector between the detector and the frontend electronics.

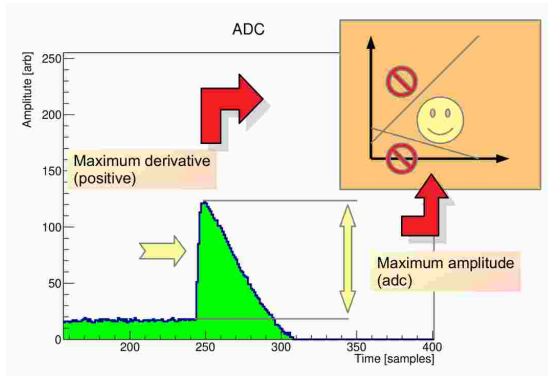


Figure 4: The idea of creating parameters on the basis of which cuts will be made to select signals from neutrons. Amplitude value signal and the maximum difference between successive samples for each pulse is marked in Fig.5

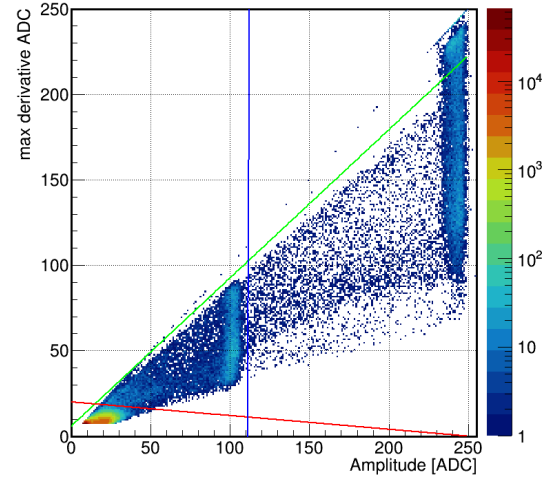


Figure 5: Practical applications of selection cuts on single counter data. Signal corresponding to neutrons are located in triangle between cuts lines. Amplitude distribution corresponding to selected signals is presented on Fig.6.

124 The Fig.6 shows the amplitude distributions recorded in a single ^3He counter after applying
 125 the selection method described earlier. The obtained amplitude distribution (green line) perfectly
 126 corresponds to the model of this type of neutron counters [5]. The peak with an ADC value of 100
 127 corresponds to the full energy peak (764 keV) of the reaction (eq. 1).

128 4. Measurement results

129 The outcome of the NEMESIS measurement is summarised in Fig.7. The ambi-
 130 ent neutron background dominates multiplicity-
 131 one events. The results with and without the Pb
 132 target differ just by 17%. For multiplicity two,
 133 background events are already suppressed by
 134 order of magnitude. The neutron spectra for
 135 multiplicity two and above show a distinct linear
 136 dependence in the log-log scale, indicating a
 137 simple power-law dependence. The fits yielded
 138 -3.15 ± 0.03 for the slope of the Pb run and
 139 -6.92 ± 2.29 for the background run. For mul-
 140 tiplicities around and above 20, the measured
 141 points fall short of the extrapolated line. This
 142 was expected, as no efficiency corrections were applied. This will be done after the completion of
 143 the simulations campaign to characterise the performance of the experimental setup.

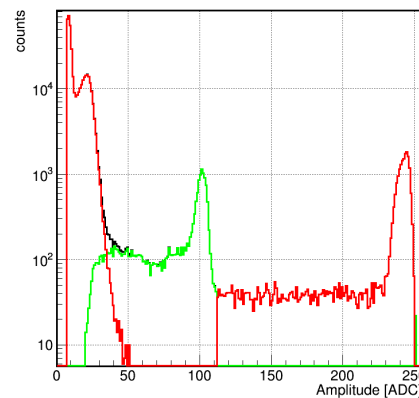


Figure 6: Amplitude spectra from single ^3He neutron counter. Green line represent neutron signals, black – all signals, red – rejected by cuts

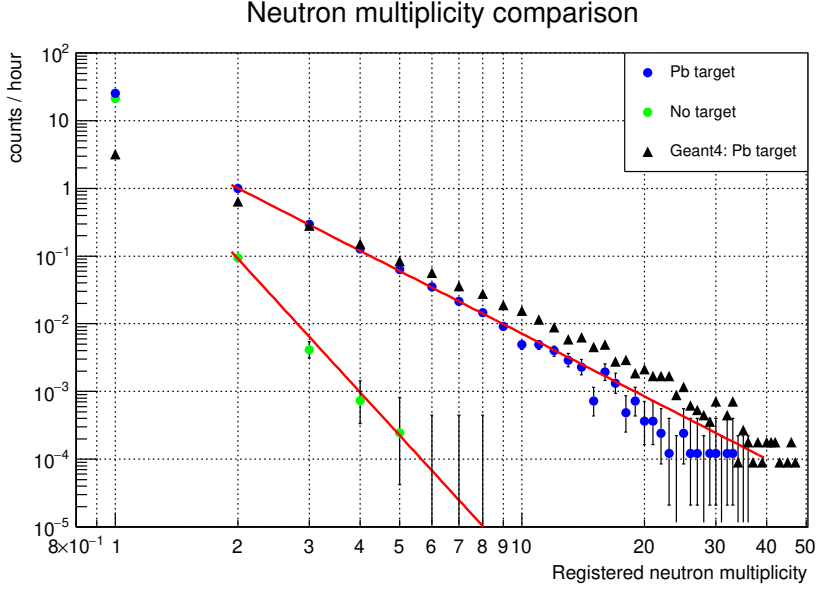


Figure 7: Registered neutron multiplicities recorded in run with lead target (blue dots), and without any target material (green dots). Black triangles correspond to results of Geant4 simulations for interactions of muons with lead target material.

145 Aspects related to possible Dark Matter annihilation signatures in NEMESIS neutron multi-
 146 plicity spectra are discussed in ICRC 2021 contribution #394 and published in the proceedings of
 147 this conference [14].

148 5. Geant4 simulations

149 We also performed Monte Carlo simulations using Geant4 [15] version 10.06.02 with
 150 QGSP_BERT_HP Physics List with thermal scattering model $S(\alpha, \beta)$ [16]. This model, impor-
 151 tant for neutrons with energies below 4 eV, considers chemically bound atoms in materials like
 152 polyethylene or water. The neutron data files for High Precision Neutron models are based on
 153 ENDF files.

154 We have performed detection efficiency simulations for a broad range of neutron energies. We
 155 expect similarity with spallation spectra with the average neutron energy around 2 MeV. Neutron
 156 registration efficiency, summed up for all counters, reaches 16% for neutron energies around 10
 157 eV, and 10% for neutrons in the $1 \div 10$ MeV range. For neutrons with energies above 10 MeV, the
 158 production of secondary neutrons from the $\text{Pb}(n, xn)$ reaction starts to play a dominant role.

159 Assuming muon distribution at sea-level from Guan et al. [17], based on the standard Gaisser's
 160 formula, and a simplified lepton propagation through matter with Muon Monte Carlo (MMC) code
 161 [18], we have simulated 50 million CR muons hitting the NEMESIS Pb target. The outcome was
 162 normalised to the well-known muon flux value of $1.29 \pm 0.06 \text{ m}^{-2} \text{ s}^{-1}$, measured previously by
 163 EMMA [3]. The best match with the measured neutron spectrum, shown in Fig.7, was obtained
 164 assuming a constant 6.6% efficiency for our setup. Because of the included simplifications, his value

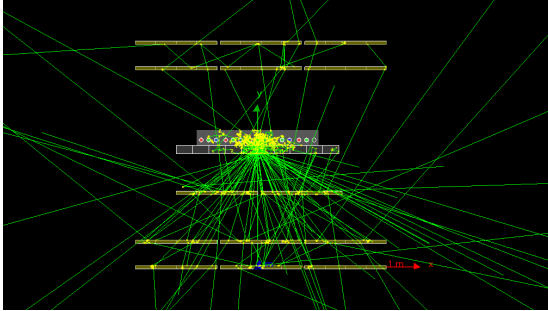


Figure 8: Geant4 schematic view presenting 100 neutron tracks for neutron transport and detection simulations. 10 MeV neutrons are emitted from the same position in lead.

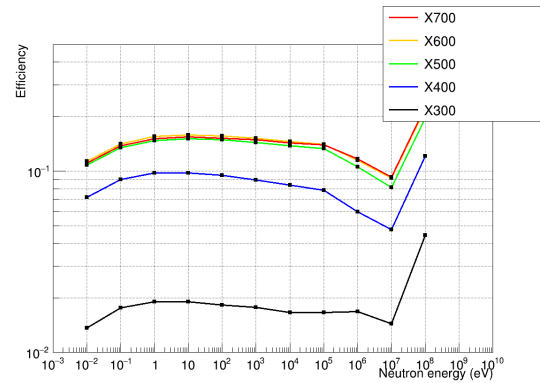


Figure 9: Simulated registration efficiency for mono-energetic neutrons by each neutron counters from the central one (X700) to the most to the side (X300).

165 represents the lower limit of NEMESIS neutron efficiency. Other preliminary estimates yielded an
 166 $8 \pm 2\%$ efficiency.

167 The presented results are preliminary. Further analysis and simulations are ongoing. We
 168 should be able to present them at the next ICRC conference.

169 6. Conclusion

170 After the first 18 months of operation, NEMESIS delivered valuable data on muon-induced
 171 neutron multiplicities and yields in lead. Data on multiplicities and yield from copper will follow.
 172 When properly analysed, the results will impact simulation software and improve the understanding
 173 of the neutron background in underground experiments.

174 The NEMESIS setup is upgradeable. As the next step, we intend to double the number of
 175 neutron detectors and increase target mass. There are plans to move simulation to the local computer
 176 clusters.

177 7. Acknowledgements

178 This work was financially supported in part by the EU (INTERREG for Baltic Sea programme)
 179 as part of the BSUIN project, and by the Polish Ministry of Science and Higher Education (grant
 180 no. 3988/INTERREG BSR/2018/2).

181 References

- 182 [1] Callio webpage: <https://callio.info>. Accessed: 2021-06-22
- 183 [2] W. H. Trzaska et al., Possibilities for Underground Physics in the Pyhäsalmi mine, 2018,
 184 [arXiv:1810.00909](https://arxiv.org/abs/1810.00909).

- 185 [3] P. Kuusiniemi et al., Performance of tracking stations of the underground cosmic-ray detector
186 array EMMA. *Astropart. Phys.*, **102**,67–76, 2018.
- 187 [4] M. Kasztelan et al., Detector Calibration and Data Acquisition System in the Roland Maze
188 Project, 2006. *ECRS 2006 Proceedings*.
- 189 [5] Z. Dębicki et al., Helium counters for low neutron flux measurements, *Astrophys. Space Sci.*
190 *Trans.*, **7**, 511-514, 2011
- 191 [6] ZdAJ-HITEC webpage: <http://hitecpoland.eu>
- 192 [7] Z. Debicki et al., Thermal neutrons at Gran Sasso. *Nucl. Phys. B Proc. Suppl.*, **196**, 429–432,
193 2009
- 194 [8] Z. Debicki et al., Neutron flux measurements in the Gran Sasso national laboratory and in the
195 Slanic Prahova Salt Mine, *Nucl. Instrum. Meth. A*, **910**, 133-138, 2018
- 196 [9] Kinga Polaczek-Grelik et al., Natural background radiation at Lab 2 of Callio Lab, Pyhäsalmi
197 mine in Finland, *Nucl. Instrum. Meth. A*, **969**, 164015, 2020
- 198 [10] BSUIN webpage: <http://bsuin.eu/> Accessed: 2021-06-28
- 199 [11] W. H. Trzaska et al. Cosmic-ray muon flux at Canfranc Underground Laboratory. *Eur. Phys.*
200 *J. C*, 79(8):721, 2019, 1902.00868.
- 201 [12] E. V. Akhrameev et al. Multi-pixel Geiger-mode avalanche photodiode and wavelength shifting
202 fibre readout of plastic scintillator counters of the EMMA underground experiment. *Nucl.*
203 *Instrum. Meth. A*, **610**, 419–422, 2009, 0901.4675
- 204 [13] Brun, R. and Rademakers, F., ROOT: An object oriented data analysis framework, doi:
205 "10.1016/S0168-9002(97)00048-X", *Nucl. Instrum. Meth. A*, Vol. **389**, 81-86, 1997
- 206 [14] W.H. Trzaska et al. New NEMESIS Results, 2021. *ICRC 2021 Proceedings*.
- 207 [15] Recent developments in Geant4, *Nucl. Instrum. Meth. A*, **835**, 2016, 186-225, ISSN 0168-9002
- 208 [16] C.T. Ballinger. The direct S(alpha,beta) method for thermal neutron scattering. *American*
209 *Nuclear Society, Inc., La Grange Park, IL (United States)*, Dec 1995.
- 210 [17] M. Guan et al., A parametrization of the cosmic-ray muon flux at sea-level,
211 <https://arxiv.org/abs/1509.06176v1>
- 212 [18] D. Chirkin et al., Propagating leptons through matter with Muon Monte Carlo (MMC).
213 <https://arxiv.org/abs/hep-ph/0407075>